Separation of Submicron Bioparticles by Dielectrophoresis

Hywel Morgan, Michael P. Hughes, and Nicolas G. Green

Bioelectronic Research Centre, Department of Electronic and Electrical Engineering, University of Glasgow, Glasgow G12 8QQ, Scotland

ABSTRACT   Submicron particles such as latex spheres and viruses can be manipulated and characterized using dielectrophoresis. By the use of appropriate microelectrode arrays, particles can be trapped or moved between regions of high or low electric fields. The magnitude and direction of the dielectrophoretic force on the particle depends on its dielectric properties, so that a heterogeneous mixture of particles can be separated to produce a more homogeneous population. In this paper the controlled separation of submicron bioparticles is demonstrated. With electrode arrays fabricated using direct write electron beam lithography, it is shown that different types of submicron latex spheres can be spatially separated. The separation occurs as a result of differences in magnitude and/or direction of the dielectrophoretic force on different populations of particles. These differences arise mainly because the surface properties of submicron particles dominate their dielectrophoretic behavior. It is also demonstrated that tobacco mosaic virus and herpes simplex virus can be manipulated and spatially separated in a microelectrode array.

INTRODUCTION

When biological particles are subjected to an AC field, a dipole moment is induced in the particle. In a diverging field the polarized particles experience a force that can cause them to move to regions of high or low electric field, depending on the particle polarizability compared with the suspending medium. This force was termed dielectrophoresis (DEP) by Pohl (1951, 1978). The magnitude of the dipole moment depends on the polarizability of the particle, and this in turn is governed by the dielectric properties of the particle and the medium (Pohl, 1978; Jones, 1995). Thus by choosing an appropriate medium conductivity and permittivity, particles of similar (but not identical) dielectric properties can be separated efficiently. For example, similar bacterial species can be separated from each other by using gradients in conductivity (Markx et al., 1996). It has also been demonstrated that leukemic cells (Becker et al., 1994), breast cancer cells (Becker et al., 1995), and CD34+ cells (Stephens et al., 1996) can be separated or enriched from human blood. Recent work has shown that submicron particles can be elegantly manipulated using dielectrophoretic methods. For example, combined electrophoretic and dielectrophoretic forces have been used to trap and manipulate DNA on planar microelectrodes (Washizu and Kurosawa, 1990; Washizu et al., 1995; Asbury and van den Engh, 1998). An efficient and effective method for the direct manipulation and separation of submicron particles could ultimately lead to the development of revolutionary methods for the analysis of biological material, using integrated microfabricated bioelectronic analysis devices, i.e., a laboratory on a chip.

In this paper we present evidence that DEP can be used as a means of separating submicron particles according to their dielectric properties. Using microfabricated electrodes, we show that at the correct frequency and medium conductivity, submicron latex particles can be separated according to their surface charge properties and that two viruses, tobacco mosaic virus and herpes simplex virus, can be separated.

THEORY

Hydrodynamics

A particle in fluid experiences a drag force, given by Stokes law as $\mathbf{F}_{\mathrm{Drag}} = -f\mathbf{v}$, where f is the friction factor of the particle. A particle less than 10 μm in diameter moving under the influence of a force $\mathbf{F}$ can be considered to always move at the terminal velocity given by $\mathbf{F}/f$. For low Reynolds numbers, the friction factor for a spherical particle is given by $f = 6\pi\eta r$, where r is the hydrodynamic radius of the particle, $\mathbf{v}$ is the particle velocity, and η is the viscosity of the medium.

Dielectrophoresis

The time-averaged DEP force is (Jones, 1995)

$$\mathbf{F}_{\mathrm{DEP}} = 2\pi r^3 \epsilon_{\mathrm{m}} \mathrm{Re}\{K(\omega)\} \nabla |E_{\mathrm{rms}}|^2 \tag{1}$$

where E_{rms} is the rms electric field, r is the particle radius, ω is the angular field frequency, and Re{ } indicates the real part of. The factor $K(\omega)$ is a measure of the effective polarizability of the particle (the Clausius-Mossotti factor), given by

$$K(\omega) = \frac{(\epsilon_{\mathrm{p}}^* - \epsilon_{\mathrm{m}}^*)}{(\epsilon_{\mathrm{p}}^* + \epsilon_{\mathrm{m}}^*)} \tag{2}$$

where ϵ_{p}^* and ϵ_{m}^* are the complex permittivities of the particle and the medium, respectively. The complex permittivity is defined as $\epsilon^* = \epsilon - j(\sigma/\omega)$, where $j = \sqrt{-1}$, ϵ is

Address reprint requests to Dr. Hywel Morgan, Bioelectronic Research Centre, Department of Electronic and Electrical Engineering, University of Glasgow, Glasgow G12 8QQ, Scotland. Tel.: 44-141-330-5237; Fax: 44-141-330-4907; E-mail: h.morgan@elec.gla.ac.uk.

the permittivity, and σ is the conductivity of the dielectric. For the case of a multishelled particle, the polarizability can be determined using the smeared-out or multishell model (Irimajiri et al., 1979; Huang et al., 1992).

The Clausius-Mossotti factor not only depends on the dielectric properties of the particle and medium, but also on the frequency of the applied field. Variations in this factor give rise to a dielectrophoretic force that is frequency dependent and unique to a particular particle type. For a sphere, the real part of $K(\omega)$ is bounded by the limits $1 < \mathrm{Re}\{K(\omega)\} < -\frac{1}{2}$ and varies with the frequency of the applied field and the complex permittivity of the medium. Positive DEP occurs when $\mathrm{Re}\{K(\omega)\} > 0$, the force is toward the high electric field, and the particles collect at the electrode edges. The converse of this is negative DEP, which occurs when $\mathrm{Re}\{K(\omega)\} < 0$, the force is in the direction of decreasing field strength, and the particles are repelled from the electrode edge.

Ignoring Brownian motion and the buoyancy force, the equation of motion can be written as

$$m \frac{d\mathbf{v}}{dt} = \mathbf{F}_{\mathrm{DEP}} - \mathbf{F}_{\mathrm{Drag}} \qquad (3)$$

For small particles (low Reynolds numbers) the instantaneous velocity is proportional to the instantaneous dielectrophoretic force, so that $\mathbf{v} = (\mathbf{F}_{\mathrm{DEP}}/f)$, or substituting for $\mathbf{F}_{\mathrm{DEP}}$,

$$\mathbf{v} = \frac{2\pi r^3 \epsilon_{\mathrm{m}} \mathrm{Re}\{K(\omega)\} \nabla |E_{\mathrm{rms}}|^2}{f} \qquad (4)$$

so that for a spherical particle the dielectrophoretic mobility is given by

$$\mathbf{u}_{\mathrm{DEP}} = \frac{r^2 \epsilon_{\mathrm{m}} \mathrm{Re}\{K(\omega)\}}{3\eta} \qquad (5)$$

in the direction of $\nabla |E|^2$. It can be seen that for a spherical particle the dielectrophoretic mobility depends on the surface area of the particle, together with the real component of the polarizability. Thus DEP could potentially be used to achieve highly controlled selective separation of particles.

Fluid heating

As indicated by Eq. 5, the dielectrophoretic mobility of a particle scales directly with the surface area, so that to manipulate small particles (<1 μm diameter), larger electric field gradients are required. The use of microfabricated electrodes as a means of generating high electric fields has meant that the dielectrophoretic movement of submicron particles has now been established beyond doubt (Washizu et al., 1994; Schnelle et al., 1996; Müller et al., 1996; Morgan and Green, 1997; Green et al., 1997). However, Joule heating of the fluid occurs, which in certain circumstance can give rise to fluid motion that generates additional Stokes forces on the particles.

For a conducting fluid, the power generated (per unit volume) is given by $W = \sigma |\mathbf{E}|^2$ (Wm^{-3}). In dielectrophoretic systems, microelectrode arrays are used so that the volume in which this heat is generated is very small, and typical power dissipation is in the range of 1–10 mW. Thermal equilibrium is achieved rapidly, within 1 ms of application of the electric field (Ramos et al., 1998), and both calculations and measurements show that for low conductivity media the steady-state temperature rise is small and not sufficient to denature biological samples.

As an example, it has been shown that for the simple case of an interdigitated electrode geometry in contact with a medium of conductivity 0.01 Sm^{-1} (with 20 V peak to peak applied), the steady-state temperature rise can be calculated to be 6°C (Ramos et al., 1998). This can be compared with a value of 2°C measured within 250 μm of the electrodes. In most cases such temperature increments are unlikely to result in the loss of biological activity. However, the temperature rise is proportional to medium conductivity, so that for 100 mM phosphate buffer ($\sigma_{\mathrm{m}} \approx 1$ Sm^{-1}), the temperature rise would approach 100°C for the same applied voltage, which is clearly sufficient to cause degradation of the sample. Reducing the dimensions of the system means that the voltage required to produce a given electric field strength is lower, and as a result both the power dissipation and the temperature increment are reduced. Thus it can clearly be seen that to achieve the controlled dielectrophoretic manipulation of submicron particles without causing a localized temperature rise, small-feature-size microelectrodes must be used.

The heat generation and dissipation are nonuniform, so that gradients in the conductivity and/or permittivity of the suspending medium occur, and these discontinuities produce volume forces on the liquid (Stratton, 1941), which are referred to as the *electrothermal force*. The conductivity gradient produces free volume charge and gives rise to the Coulomb force, and the permittivity gradient produces the dielectric force. In different frequency ranges either the Coulomb or the dielectric force dominates, and the transition from one to the other occurs at a frequency f_{c}, given by (Ramos et al., 1998)

$$\omega_{\mathrm{c}} = 2\pi f_{\mathrm{c}} \approx \frac{1}{\tau} \left(2 \frac{\left| \dfrac{\partial \sigma}{\sigma \partial T} \right|}{\left| \dfrac{\partial \epsilon}{\epsilon \partial T} \right|} \right)^{1/2} \qquad (6)$$

where $\tau = (\epsilon/\sigma)$ is the charge relaxation time of the liquid; $(1/\sigma)(\partial \sigma/\delta T)$ and $(1/\epsilon)(\partial \epsilon/\delta T)$ are the normalized temperature dependence of the conductivity and permittivity of the medium, respectively. (For water, $(1/\sigma)(\partial \sigma/\delta T) = +2\%$ per degree and $(1/\epsilon)(\partial \epsilon/\delta T) = -0.4\%$ per degree (Lide, 1994).) At the frequency given by Eq. 6, the electrothermal force will have a minimal effect on the dielectrophoretic manipulation/separation of the particles. Thus optimal separation of submicron particles can be achieved by choosing a frequency at or close to f_{c}.

MATERIALS AND METHODS

Electrode fabrication

For particle manipulation and separation, electrodes of the polynomial and castellated design were used (Huang and Pethig, 1991; Price et al., 1988; Pethig et al., 1992). Electrodes were constructed on glass substrates, using direct-write electron beam lithography. The electrodes were fabricated by writing the pattern onto quartz mask plates (Hoya), using a Leica EBPG HR5 beamwriter, operating at 50 kV. After development of the resist, metal (titanium/palladium/gold) was evaporated onto the exposed mask plate. Lift-off in acetone was used to complete the electrode. Although the dimensions of the electrodes are not submicron, electron beam lithographic methods guarantee precise and controlled electrode geometry at 50-nm scale resolution, so that the electric field configuration is well reproduced.

Photographs of the two electrodes used in this work are shown in Fig. 1. The polynomial electrode is shown in Fig. 1 *a*, and this design generates a high electric field along all of the electrode edges, with a minimum in the field at the center. Thus particles experiencing positive DEP will move to the electrode edges, and those experiencing negative DEP will move into the center, where, if they have negative buoyancy, they will remain trapped. The castellated electrodes (Fig. 1 *b*) produce regions of high electric field along the tips of the castellations and well-defined regions of minimum electric field in the bays between the tips, as shown in the figure. Further details of the 3-D electric field distribution for these electrodes have been published elsewhere (Wang et al., 1993; Green et al., 1997; Green and Morgan, 1997).

Latex spheres

Carboxylate-modified latex spheres were obtained from Molecular Probes (Eugene, OR). The spheres had a net negative charge and were supplied preloaded with a fluorescent dye. Particles with diameters of 216, 282, and 557 nm were used as supplied by the manufacturer and resuspended in 0.1 mM KCl at a particle concentration of 2×10^{-6} v/v.

For some experiments a monolayer of protein (IgG) was immobilized on the latex particles according to the following method. Two hundred fifty microliters of microspheres at 2% w/v was mixed with 500 μl of 10% (w/v) 1-ethyl-3-(3-dimethylaminopropyl) carbodiimide (EDAC) solution and 250 μl 50 mM KH_2PO_4. The solution was incubated for 30 min at room temperature, then dialyzed against 0.1 M Borax solution for 1 h. Two hundred fifty microliters of 10 mg/ml protein (mouse IgG) was then added to the dialyzed spheres, and the solution was incubated for 2–4 h at room temperature. One hundred microliters of 1 M glycine was added to stop the reaction, and the protein-functionalized spheres were further purified, by either centrifugation or dialysis.

Virus preparation

Tobacco mosaic virus (TMV) and herpes simplex virus (HSV) type 1 were used as model biological particles. TMV is a plant virus; it is a 280-nm-long protein tube surrounding a core of RNA (Mathews, 1981). HSV-1 is one of the largest mammalian viruses and is a spherical enveloped DNA-containing particle of $\sim$250 nm diameter (Whitley, 1996). The preparation and fluorescent labeling of both TMV and HSV has been reported elsewhere (Green et al., 1997; Hughes et al., 1998).

Dielectrophoresis separation experiments

Particles for DEP separation experiments were prepared from stock solution by centrifugation and resuspension in an appropriate buffer. A microliter volume chamber was constructed around the electrode, using glass spacers and adhesives. The chamber had a depth of $\sim$50 μm and a sample volume on the order of 1 μl. Virus solution was pipetted into the chamber, and the assembly was sealed with a coverslip. The electrodes were energized using a signal generator providing 20-V peak-to-peak sinusoidal signals over the frequency range 1 kHz to 20 MHz. Potentials were applied
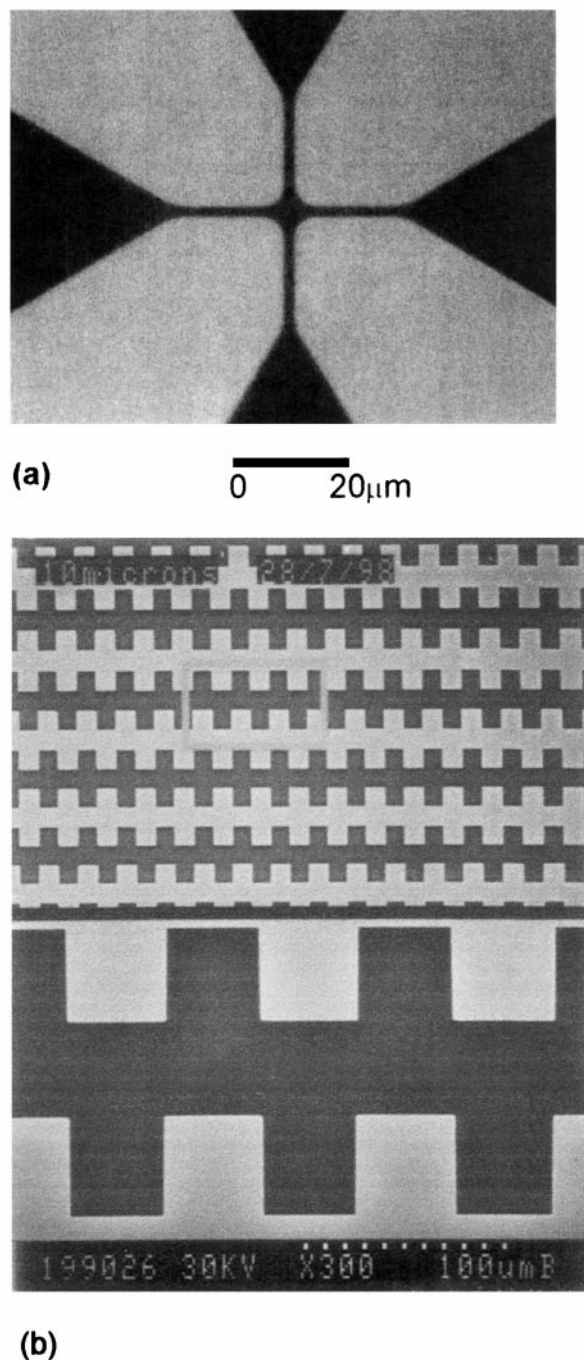

(a)

(b)

FIGURE 1 Photograph showing the two types of electrodes used in this work. (*a*) A polynomial electrode. (*b*) A section of the repeat pattern of a castellated electrode. The electrodes are fabricated using direct write electron beam lithography and consist of a Ti/Pd/Au layer on a glass substrate. The dimensions of the polynomial electrode are 2 μm between adjacent arms and 6 μm across the center, and the characteristic dimensions of the castellations vary between 1 and 15 μm.

with a 180° phase difference between adjacent electrodes. Particle movement was observed with a Nikon Microphot microscope, a Photonic Science Isis II image-intensifying camera, and a Sony S-VHS video recorder. Photographs were also taken with 3200 ASA color film. Conductivity measurements were performed with a Hewlett-Packard 4192A impedance analyzer and a Sentek conductivity cell in the frequency range 100 kHz to 1 MHz.

DEP force calculations

Latex particles

The dielectrophoretic response of the latex particle is governed by the Clausius-Mossotti factor (Eq. 2). For submicron particles the response is dominated by the particle conductivity, which in turn is governed by the surface charge on the particle. The conductivity of a latex particle can be written as the sum of the bulk conductivity and the surface conductivity, i.e., $\sigma_p = \sigma_b + (2K_s/r)$ (Arnold et al., 1987), where K_s is the surface conductance and σ_b is the bulk conductivity (approximately zero for latex). The surface conductivity of the three sizes of particles used in this work have been calculated previously (Green and Morgan, 1997; Green and Morgan, 1999), so that by using Eq. 2, the polarizability and thus the force on each particle can be calculated. Fig. 2 *a* shows the frequency dependence of the Clausius-Mossotti factor for the 216-nm and 557-nm particles with the particle permittivity $\epsilon_p = 2.55$ and a medium conductivity $\sigma_m = 1 \text{ mSm}^{-1}$. For this calculation the surface conductance of the particle was
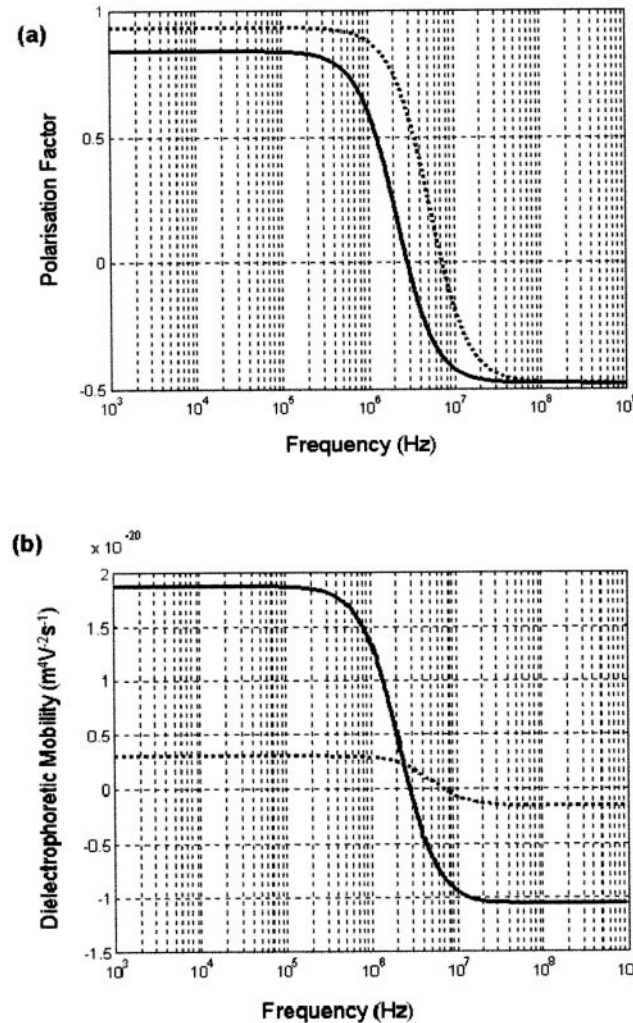
set at 2.32 nS. It can be seen that in the frequency range between 3 and 7 MHz, the 216-nm particles experience positive DEP, whereas the 557-nm particles experience negative DEP, so that the two particle types could be spatially separated. Although the polarization factor for the 216-nm particle is greater, it can be seen from Fig. 2 *b* that the dielectrophoretic mobility is greater for the 557-nm particle. Thus in a dynamic flow-through separation system with constant field gradient (and at low frequencies), the larger particles would elute ahead of the smaller particles.

Virus

HSV is a spherical enveloped particle, and consequently the frequency-dependent force on the particle follows the trend predicted using the single-shell model (Hughes et al., 1998) and Eq. 2. TMV is rod-shaped, and in this case, assuming that the particle is aligned with the field, the DEP force can be written as (Morgan and Green, 1997)

$$\mathbf{F}_{\text{DEP}} = \frac{\pi a^2 b}{3}\, \epsilon_m \text{Re}\left\{\frac{\epsilon_p^* - \epsilon_m^*}{\epsilon_m^*}\right\} \nabla |\mathbf{E}|^2 \qquad (7)$$

where a is the radius of the rod and b is the half-length.

It has been shown that the TMV particle can be approximated to a solid homogeneous dielectric cylinder with a particle relative permittivity $\epsilon_p = 55$ and conductivity $\sigma_p = 0.085 \text{ Sm}^{-1}$ (Morgan and Green, 1997). In contrast, HSV consists of a conducting core surrounded by an insulating membrane (similar to a cell). Experiments have shown (Hughes et al., 1998) that to a first approximation HSV can be modeled as a single-shelled dielectric sphere, with an internal permittivity $\epsilon_i = 70$ and conductivity $\sigma_i = 8 \text{ mSm}^{-1}$, surrounded by an insulating membrane with a permittivity $\epsilon_{\text{mem}} = 10$, bulk conductivity $\sigma_{\text{mem}} \leq 10^{-8} \text{ Sm}^{-1}$, and surface conductance $K_s = 3.5 \text{ nS}$.

Using the above parameters, a plot of the frequency variation of the polarization factor, estimated from Eq. 2 for HSV and Eq. 7 for TMV, was calculated as a function of frequency at a medium conductivity of 10 mSm^{-1}. The results are shown in Fig. 3. It can be seen that in the frequency range shown, the force on the TMV remains positive (the virus is always more polarizable than the medium), whereas for HSV for frequencies up to 4 MHz the force is positive but then goes negative. Although this figure

FIGURE 2 (*a*) A plot of the Clausius-Mossotti factor versus frequency for 216-nm- (– – –) and 557-nm-diameter (——) latex particles with a particle permittivity $\epsilon_p = 2.55$ and a medium conductivity $\sigma_m = 1 \text{ mSm}^{-1}$. The surface conductance was set at 2.32 nS for both particles. (*b*) A plot of the dielectrophoretic mobility for the 216-nm- (– – –) and 557-nm-diameter (——) particles calculated from Eq. 5. Particle permittivity $\epsilon_p = 2.55$, and medium conductivity $\sigma_m = 1 \text{ mSm}^{-1}$. The surface conductance was set at 2.32 nS for both particles.
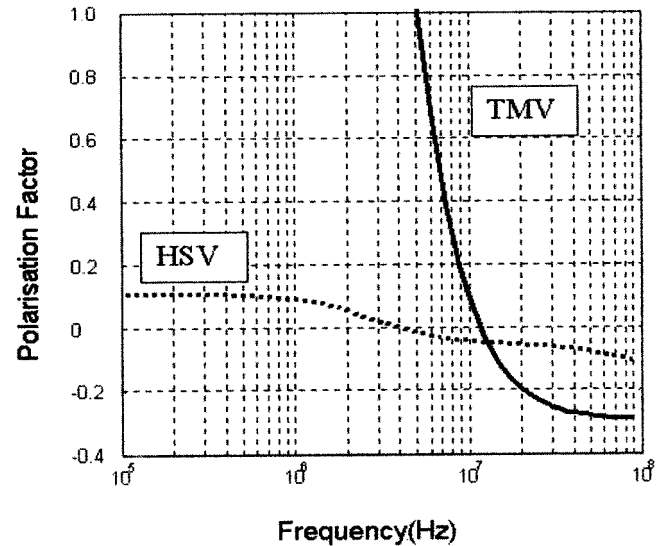
FIGURE 3 A plot of the Clausius-Mossotti factor versus frequency for TMV and HSV with a medium conductivity $\sigma_m = 10 \text{ mSm}^{-1}$. For details of the dielectric models and parameters, see text. This figure illustrates that at a frequency of 4–10 MHz, HSV experiences negative DEP, whereas TMV experiences positive DEP, so that both viruses can be separated using an appropriate electrode.

does not show the absolute force on the virus particles, it does represent the direction and frequency variation of the force. This figure shows that for any frequency in the range 4–10 MHz, the two viruses should respond in completely different directions to the electric field, with TMV experiencing positive DEP and HSV experiencing negative DEP, implying that the spatial separation of the two species should be possible.

RESULTS

Dielectrophoretic manipulation

Latex particles

The frequency-dependent dielectrophoretic properties of submicron latex particles have been well characterized (Green and Morgan, 1997, 1999). Their response is dominated by surface charge effects, and at low conductivities the particles exhibit almost exclusively positive DEP, changing to negative DEP at frequencies above the Maxwell-Wagner interfacial relaxation time. The dielectrophoretic trapping of both 216-nm and 282-nm latex particles in a castellated electrode array is demonstrated in Fig. 4. For this experiment particles were suspended in KCl of conductivity 250 μSm^{-1}. At an applied frequency of 1 MHz and a potential of 10 V peak to peak, positive DEP collection of 282-nm particles occurred as shown in Fig. 4 a. In this case the electrodes had a feature size of 14 μm across one tip. The particles are attracted to the high-field regions of the electrode array, and pearl chaining due to dipole-dipole interaction can clearly be seen in this figure. In an electrode of 8 μm characteristic dimension, an applied voltage of 10 V peak to peak and a frequency of 6 MHz, the 216-nm-diameter particles experience negative DEP and can be trapped in the electrode bays, where the electric field is a minimum. An example of this is shown in Fig. 4 b, where the beads can be seen forming small triangular aggregates. The behavior of such particles in castellated electrodes is similar to that reported by other workers for larger (>1-μm diameter) particles (Pethig et al., 1992) and indicates that under correct conditions, Brownian motion is not a "disruptive" force for the controlled manipulation of submicron particles.

Virus

The frequency-dependent dielectrophoretic behavior of both HSV and TMV has been reported previously (Hughes et al., 1998; Morgan and Green, 1997). For the electrolyte conductivity used in these experiments, 10 mSm^{-1}, TMV experienced positive DEP and collected at the high electric field regions, which for the polynomial electrodes corresponded to the interelectrode gaps. A photograph of TMV collecting in this manner is shown in Fig. 5 a. Here the applied potential was 5 V peak to peak at a frequency of 6 MHz. The virus collects within seconds of application of the field and rapidly diffuses away when the field is switched off.

At the same medium conductivity and at a frequency of 6 MHz, HSV experiences weak negative DEP. A fluorescence micrograph showing trapping of HSV under negative DEP
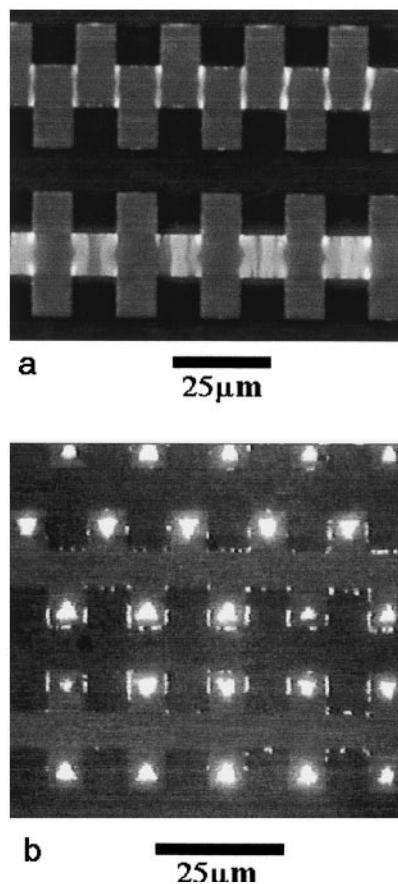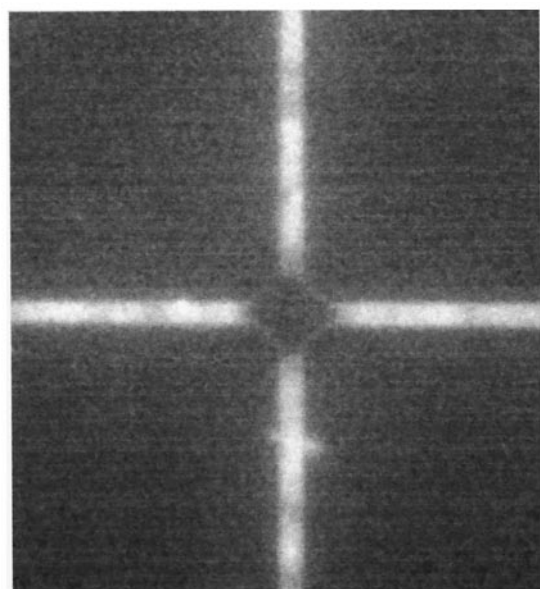

a 25μm

b 25μm

FIGURE 4 (a) A captured video image showing 282-nm-diameter latex particles experiencing positive DEP on a castellated microelectrode array with characteristic dimensions of 14 μm from tip to tip. The medium was KCl of conductivity 250 μSm^{-1}, the applied voltage was 10 V peak to peak, and the frequency was 1 MHz. The particles can clearly be seen to be attracted to the electrode tips and to form long pearl chains between opposing electrode tips. (b) A captured video image showing 216-nm-diameter latex particles experiencing negative DEP and collecting in triangular aggregates in the low-field regions of a castellated microelectrode array with characteristic dimensions of 8 μm. The medium was KCl of conductivity 250 μSm^{-1}, the applied voltage was 10 V peak to peak, and the frequency was 6 MHz.

in the center of a polynomial electrode is shown in Fig. 5 b. If the frequency is reduced to below 4 MHz, the virus moves to the regions of higher electric field under the influence of positive DEP, as shown in Fig. 5 a for the TMV.
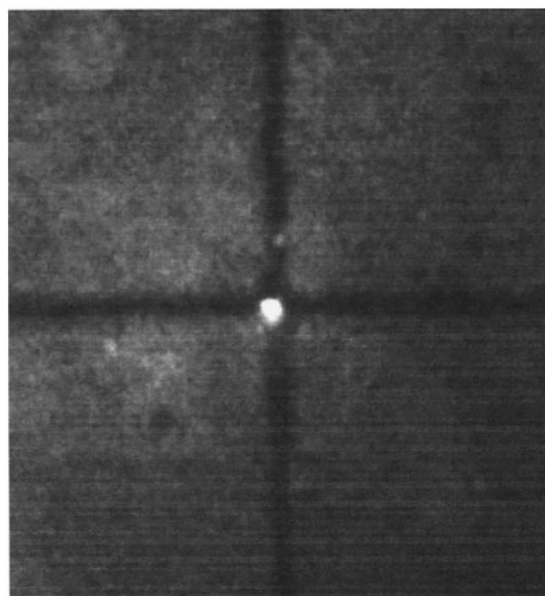
Dielectrophoretic separation

Latex particles

At a suitable frequency and applied potential, it was possible to spatially separate a mixture of latex particles into two distinct populations. This can clearly be seen in Fig. 6 a, which shows 216-nm- and 557-nm-diameter latex particles separating in a 10-μm feature size castellated electrode array at an applied potential of 10 V peak to peak. At a medium conductivity of 250 μSm^{-1} and frequency of 2 MHz, one type of particle experiences positive DEP,

(a)

(b)

0   20 μm

FIGURE 5 Captured video images showing fluorescently labeled virus collecting on a polynomial electrode. In *a*, tobacco mosaic virus (TMV) can be seen collecting under positive DEP at the high-field regions of a polynomial electrode. In *b*, herpes simplex virus type 1 (HSV-1) is trapped under negative DEP in the low-field region at the center of the electrode. The frequency was 6 MHz, the medium conductivity was 10 mSm^{-1}, and the applied voltage was 5 V peak to peak in both cases.

whereas the other experiences negative DEP, so that they move in diametrically opposite directions. In this case the red 216-nm spheres can clearly be seen experiencing positive DEP and forming pearl chains between opposing electrode tips, while simultaneously the green 557-nm particles experience negative DEP and are trapped in triangular patterns in the interelectrode bays.

Although this image shows that submicron particles can be spatially separated into regions of positive and negative dielectrophoretic potential energy, it is also possible to demonstrate that a variation in the magnitude of the dielectrophoretic force can also lead to the separation of particles. The dielectrophoretic properties of 216-nm beads change after immobilization of a layer of protein on the surface (Hughes et al., 1999). At low frequencies (<1 MHz) the dielectrophoretic force is positive on both labeled and unlabeled particles, but the force exerted on the labeled particle is less than on the unlabeled. Two populations of differently colored 216-nm spheres were placed on a castellated electrode array. One population (*red*) was labeled with IgG (at a surface density corresponding to monolayer coverage; Hughes et al., 1999), and the other (*green*) was used directly without surface modification. The beads were suspended in an electrolyte of conductivity 250 μSm^{-1}, and when a potential of 10 V peak to peak and a frequency of 1 MHz were applied, the green beads were strongly attracted to the electrodes, whereas the red beads were only weakly attracted. This is shown in the photograph of Fig. 6 *b*, where the green unlabeled beads can be seen at the electrode tips, whereas the red protein-coated beads form a diffuse cloud between opposite electrodes.

Virus

To demonstrate the separation of the two virus types, a mixture (~70/30% v/v) of TMV and HSV was suspended in an electrolyte of conductivity 10 mSm^{-1}. This solution was applied to a polynomial electrode with a center-to-center gap of 6 μm and a minimum spacing between opposite electrodes of 2 μm. Application of a voltage of 5 V peak to peak at a frequency of 6 MHz resulted in a physical separation of the two particle types. A schematic diagram illustrating this effect is shown in Fig. 7 *a*, together with a photograph of a typical separation experiment in Fig. 7 *b*. This photograph shows the TMV (*red*) experiencing positive DEP and collecting at the high field regions in the arms of the electrodes, while simultaneously the HSV (*green/yellow*) collects under negative DEP at the field minimum in the center of the electrode. Even though the force on the two particle types is very small, this photograph clearly shows that it is possible to produce simultaneous trapping of the HSV under negative DEP and TMV under positive DEP.

DISCUSSION

The separation of large particles and cells by DEP has been demonstrated by a number of research groups. For example,
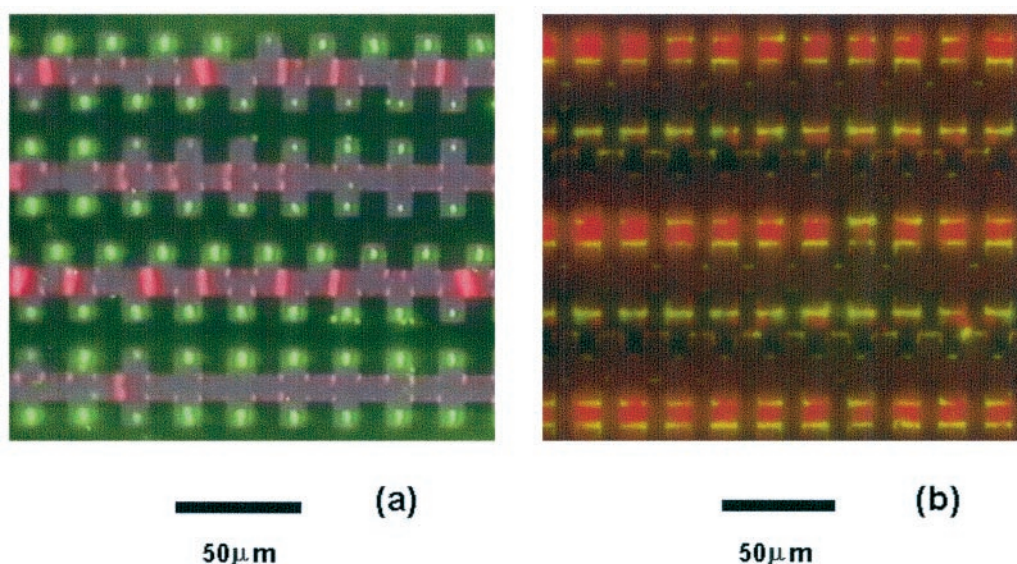
FIGURE 6 (*a*) A video image showing 216-nm- and 557-nm-diameter latex particles separating on a 10-μm castellated electrode. The red 216-nm spheres experience positive DEP and form pearl chains between opposing electrode tips, while simultaneously the green 557-nm particles experience negative DEP and become trapped in triangular patterns in the interelectrode bays. The applied potential was 10 V peak to peak at a frequency of 2 MHz, and the medium conductivity was 250 μSm^{-1}. (*b*) Captured video image of differently colored 216-nm-diameter latex spheres separating on a castellated electrode array. The red beads were coated with a monolayer of IgG, whereas the green beads was used directly without surface modification. The electrolyte conductivity was 250 μSm^{-1}, and the applied potential was 10 V peak to peak at a frequency of 2 MHz. The image shows the unlabeled green beads strongly attracted to the electrodes, whereas the red beads are only weakly attracted and form pearl chains between opposing electrode tips.

the spatial separation of particles on a microelectrode structure has been demonstrated for a range of microorganisms (Wang et al., 1993; Markx et al., 1994b) and mammalian cells (Becker et al., 1994; Gascoyne et al., 1992). Batch separation methods have been proposed in which weakly held particles are carried out of the electrode system by fluid flow (Markx and Pethig, 1995; Markx et al., 1996; Talary et

al., 1995). Furthermore, DEP combined with field-flow fractionation methods have been employed for continuous particle separation systems (Markx et al., 1997; Wang et al., 1998). The combination of field-flow fractionation with DEP has recently been demonstrated to be a useful method for enhancing the separation efficiency of a particle separator. Indeed, Washizu et al. (1994) used a combination of
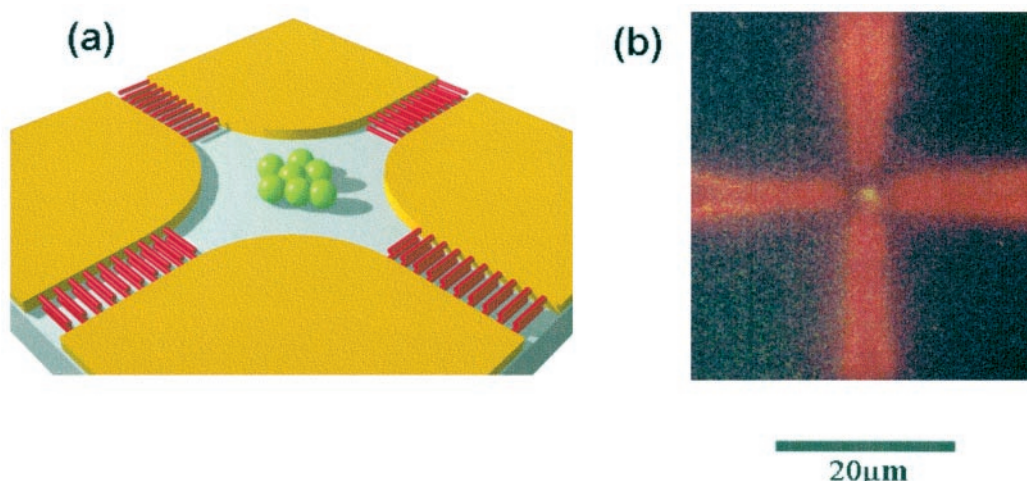

FIGURE 7 A photograph and diagram illustrating the separation of TMV and HSV in a polynomial electrode. The HSV is trapped under negative DEP forces at the field minimum in the center of the electrode array, while simultaneously TMV experiences positive DEP and collects at the high-field regions at the electrode edges, resulting in the physical separation of the two particle types. This is illustrated schematically in *a*; the photograph appears in *b*. The TMV (labeled with rhodamine B) can be seen as a red glow in the arms of the electrodes, and the green/yellow HSV (labeled with NBD-dihexadecylamine) is visible in the center of the electrode. Both viruses were suspended in an electrolyte of conductivity 10 mSm^{-1}, and the applied potential was 5 V peak to peak at a frequency of 6 MHz.

dielectrophoretic forces and fluid flow to demonstrate separation of proteins. More recently, the controlled separation of a range of micron-sized latex particles with differing surface functionality has been demonstrated through combined DEP and gravitational field-flow fractionation methods (Wang et al., 1998).

In the original work of Davis and Giddings (1986) it was proposed that field-flow fractionation could be used in combination with DEP forces and diffusion forces to separate submicron particles. For a collection of submicron particles in equilibrium, the effects of Brownian motion give rise to an additional energy that can disturb the system. Until recently it was considered that the deterministic movement of submicron particles by dielectrophoretic forces alone could not be achieved at realizable electric field strengths (Pohl, 1978). This presumption was based on the argument that the force required to move submicron particles had to overcome a diffusion barrier. However, it has now been shown that even proteins can be manipulated by dielectrophoretic forces (Washizu et al., 1994). To control the movement of particles smaller than 1 μm, the applied force must be of sufficient magnitude such that the force that arises from the thermal energy of the system (and which gives rise to Brownian motion) is of secondary importance.

In this work we have shown that the positive and negative dielectrophoretic collection of submicron particles can be accomplished by using suitable electrode arrays and that the general behavior is similar to that reported for larger particles. For example, at the correct frequencies and voltages particles can be seen to collect at the high electric field regions of electrode edges and to form pearl chains (Fig. 4 *a*). At higher frequencies particles can also be trapped by negative dielectrophoretic forces in small triangular aggregates (Fig. 4 *b*) similar to the patterns reported for larger particles such as cells and bacteria (Pethig et al., 1992).

Significantly, through appropriate choice of medium conductivity, applied frequency, and voltage, the photographs of Figs. 6 and 7 show that submicron particles and viruses can be spatially separated on a microelectrode array. However, the successful manipulation of such small particles does require the use of high electric fields generated in small volumes, which inevitably leads to the generation of heat in the system. Although natural convection is negligible (Ramos et al., 1998), the high electric field gives rise to volume forces on the liquid (the electrothermal force). Generally at field strengths in the range of 10^5 to 10^6 Vm^{-1}, our observations indicate that although these forces are present and give rise to fluid motion, the influence is less than the dielectrophoretic force acting on the particles (Ramos et al., 1998).

Theoretical predictions indicate that the electrothermal force should tend to zero at a frequency corresponding approximately to the charge relaxation time of the liquid, given exactly by Eq. 6. Thus if dielectrophoretic separation were to be performed at this frequency, the electrothermally induced fluid flow would be eliminated. To illustrate this point, a plot of the frequency variation of the "degree of

separation" between two different submicron latex particles can be constructed (Fig. 8). This plot was generated from the data shown in Fig. 2 for the 216-nm- and 557-nm-diameter particles. The plot is constructed such that if both spheres experience either positive or negative DEP, then the *y* axis ("degree of separation") is set to zero. Otherwise the magnitude of Re$\{[K_A(\omega) - K_B(\omega)]\}$ is plotted. It can be seen that there is a narrow window of conductivity and frequency over which the spheres would move in opposite directions.

Although this plot shows that separation is possible, fluid movement could dominate the DEP force so that practical separation becomes impossible. However, the separation conditions can be optimized for any given conductivity by choosing a frequency for separation given by f_c of Eq. 6, such that the electrothermally driven fluid flow is zero. Fig. 9 shows the "degree of separation" calculated at this frequency for a range of conductivities. It can be seen that in the conductivity range between $\sim$4 and 11 mSm^{-1} the electrothermal force is zero and the difference in polarizabilities is at maximum, so that separation conditions would be optimal.

In addition to demonstrating that the separation of latex beads can occur through dielectrophoretic forces, Fig. 7 *b* shows that it is possible to separate two different viral types along the same principles. Furthermore, we have also separated viruses (both TMV and HSV) from latex particles but have been unable to photograph the result, because the fluorescence intensity of the latex particles dominates over the virus.

The ability to directly separate particles on a microelectrode implies that new dielectrophoretic separation systems could be developed for submicron particles. In this work we have shown (Fig. 6 *b*) that submicron latex particles of differing dielectrophoretic mobilities can be spatially separated on a microelectrode array. Although this demonstrates a difference in the positive DEP force, Fig. 2, *a* and *b*,
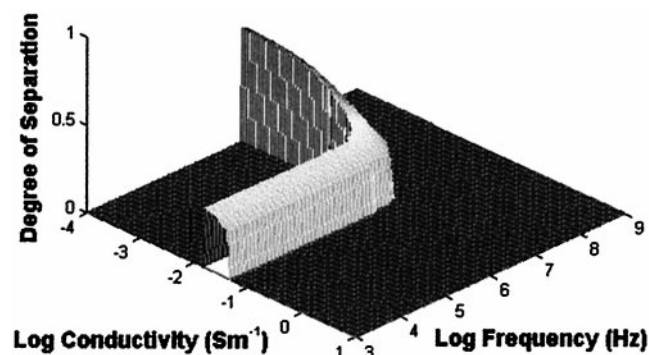

FIGURE 8 A plot of the frequency variation of the "degree of separation" between 216-nm- and 557-nm-diameter latex particles, with a particle permittivity $\epsilon_p = 2.55$ and the surface conductance set at 2.32 nS for both particles. The plot shows the magnitude of Re$\{[K_A(\omega) - K_B(\omega)]\}$ plotted as a function of conductivity and frequency. It can be seen that there is a narrow window of conductivity and frequency over which the spheres would move in opposite directions.
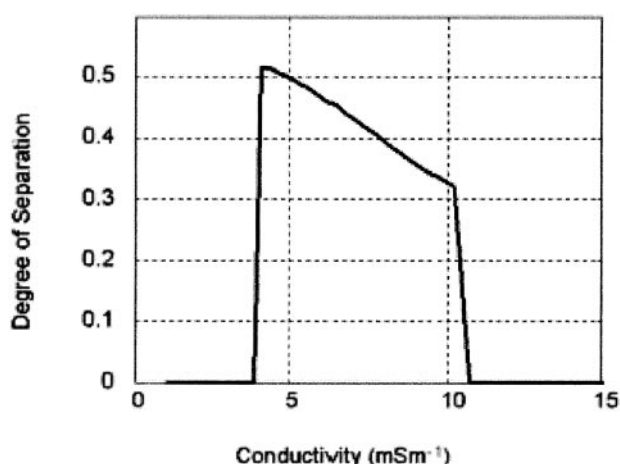
FIGURE 9   A plot showing the "degree of separation" for the 557-nm- and 216-nm-diameter latex particles plotted along a line delineated by the frequency of zero electrothermal force (Eq. 6). It can be seen that in the conductivity range of 4–10.5 mSm^{-1}, the electrothermal force is zero and the difference in polarizabilities is at maximum, so that separation conditions would be optimal.

shows that the negative DEP force varies equally with the properties of the particles. These results imply that a combination of DEP and other force fields such as fluid flow and gravitational/buoyancy forces could be employed to develop new systems for the continuous separation of submicron particles.

CONCLUSION

This work demonstrates that dielectrophoresis can be used as a means of manipulating and separating submicron particles on microelectrode arrays. In the absence of significant fluid flow, the particles behave in a reproducible manner, similar to that reported for larger particles such as cells and bacteria. It has been demonstrated that with an appropriate electrode array and a suitable electric field and frequency, separation of particles can be accomplished. Submicron latex spheres with different charge densities can be separated according to the sign and/or magnitude of the dielectrophoretic force. Separation of TMV and HSV has been demonstrated using polynomial electrodes. The results point to the possibility of producing new technologies for separating submicron bioparticles based on differences in particle polarizabilities. Systems for batch or continuous separation have been devised and implemented for microorganisms and cells, and it is conceivable that these systems could be scaled down to achieve separation of a range of submicron particles of biological relevance such as viruses, chromosomes, DNA, and macromolecules.

REFERENCES

Arnold, W. M., H. P. Schwan, and U. Zimmermann. 1987. Surface conductance and other properties of latex particles measured by electrorotation. *J. Phys. Chem.* 91:5093–5098.

Asbury, C. L., and G. van den Engh. 1998. Trapping of DNA in nonuniform oscillating electric fields. *Biophys. J.* 74:1024–1030.

Becker, F. F., X.-B. Wang, Y. Huang, R. Pethig, J. Vykoukal, and P. R. C. Gascoyne. 1994. The removal of human leukaemia cells from blood using interdigitated microelectrodes. *J. Phys. D Appl. Phys.* 27: 2659–2662.

Becker, F. F., X.-B. Wang, Y. Huang, R. Pethig, J. Vykoukal, and P. R. C. Gascoyne. 1995. Separation of human breast cancer cells from blood by differential dielectric affinity. *Proc. Natl. Acad. Sci. USA.* 92:860–864.

Davis, J. M., and J. C. Giddings. 1986. Feasibility study of dielectric field-flow fractionation. *Sep. Sci. Technol.* 21:969–989.

Gascoyne, P. R. C., Y. Huang, R. Pethig, J. Vykoukal, and F. F. Becker. 1992. Dielectrophoretic separation of mammalian cells studied by computerized image analysis. *Meas. Sci. Technol.* 3:439–445.

Green, N. G., and H. Morgan. 1997. Dielectrophoretic investigations of submicrometre latex spheres. *J. Phys. D Appl. Phys.* 30:2626–2633.

Green, N. G., and H. Morgan. 1999. Dielectrophoresis of sub-micrometre latex spheres. Part I: experimental results. *J. Phys. Chem. B.* 103:41–50.

Green, N. G., H. Morgan, and J. J. Milner. 1997. Manipulation and trapping of submicron bioparticles using dielectrophoresis. *J. Biochem. Biophys. Methods.* 35:89–102.

Huang, Y., R. Holzel, R. Pethig, and X.-B. Wang. 1992. Differences in the AC electrodynamics of viable and non-viable yeast cells determined through combined dielectrophoresis and electrorotation studies. *Phys. Med. Biol.* 37:1499–1517.

Huang, Y., and R. Pethig. 1991. Electrode design for negative dielectrophoresis applications. *Meas. Sci. Technol.* 2:1142–1146.

Hughes, M. P., M. Flynn, and H. Morgan. 1999. Dielectrophoretic measurements of sub-micrometre latex particles following surface modification. *In* Proceedings of Electrostatics '99.

Hughes, M. P., H. Morgan, F. J. Rixon, J. P. H. Burt, and R. Pethig. 1998. Manipulation of herpes simplex virus type 1 by dielectrophoresis. *Biochim. Biophys. Acta.* 1425:119–126.

Irimajiri, A., T. Hanai, and A. Inouye. 1979. A dielectric theory of "multi-stratified shell" model with its application to a lymphoma cell. *J. Theor. Biol.* 78:251–269.

Jones, T. B. 1995. Electromechanics of Particles. Cambridge University Press, Cambridge.

Lide, D. R., editor. 1994. CRC Handbook of Chemistry and Physics, 74th Ed. CRC Press, London.

Mathews, R. E. F. 1981. Plant Virology. Academic Press, London.

Markx, G. H., P. A. Dyda, and R. Pethig. 1996. Dielectrophoretic separation of bacteria using a conductivity gradient. *J. Biotechnol.* 51:175–180.

Markx, G. H., Y. Huang, X. F. Zhou, and R. Pethig. 1994a. Dielectrophoretic characterisation and separation of micro-organisms. *Microbiol. UK.* 140:585–591.

Markx, G. H., and R. Pethig. 1995. Dielectrophoretic separation of cells: continuous separation. *Biotechnol. Bioeng.* 45:337–343.

Markx, G. H., J. Rousselet, and R. Pethig. 1997. DEP-FFF: field-flow fractionation using non-uniform electric fields. *J. Liquid Chromatogr. Related Technol.* 20:2857–2872.

Markx, G. H., M. S. Talary, and R. Pethig. 1994b. Separation of viable and non-viable yeast using dielectrophoresis. *J. Biotechnol.* 32:29–37.

Morgan, H., and N. G. Green. 1997. Dielectrophoretic manipulation of rod-shaped viral particles. *J. Electrostatics.* 42:279–293.

Müller, T., A. Gerardino, T. Schnelle, S. G. Shirley, F. Bordoni, G. De Gasperis, R. Leoni, and G. Fuhr. 1996. Trapping of micrometre and sub-micrometre particles by high-frequency electric fields and hydrodynamic forces. *J. Phys. D Appl. Phys.* 29:340–349.

Pethig, R., Y. Huang, X.-B. Wang, and J. P. H. Burt. 1992. Positive and negative dielectrophoretic collection of colloidal particles using interdigitated castellated microelectrodes. *J. Phys. D Appl. Phys.* 24: 881–888.

Pohl, H. A. 1951. The motion and precipitation of suspensoids in divergent electric fields. *J. Appl. Phys.* 22:869–871.

Pohl, H. A. 1978. Dielectrophoresis. Cambridge University Press, Cambridge.

Price, J. A. R., J. P. H. Burt, and R. Pethig. 1988. Applications of a new optical technique for measuring the dielectrophoretic behaviour of micro-organisms. *Biochim. Biophys. Acta.* 964:221–230.

Ramos, A., H. Morgan, N. G. Green, and A. Castellanos. 1998. AC electrokinetics: a review of forces in microelectrode structures. *J. Phys. D Appl. Phys.* 31:2338–2353.

Schnelle, T., S. Muller, S. Fiedler, G. Shirely, K. Ludwig, A. Hermann, and G. Fuhr. 1996. Trapping of viruses in high-frequency electric field cages. *Naturwissenschaften.* 83:172–176.

Stephens, M., M. S. Talary, R. Pethig, A. K. Burnett, and K. I. Mills. 1996. The dielectrophoretic enrichment of CD34+ cells from peripheral blood stem-cell harvests. *Bone Marrow Transplant.* 18:777–782.

Stratton, J. A. 1941. Electromagnetic Theory. McGraw-Hill, New York.

Talary, M., K. I. Mills, T. Hoy, A. K. Burnett, and R. Pethig. 1995. Dielectrophoretic separation and enrichment of CD34+ cell subpopulations from bone marrow and peripheral blood stem cells. *Med. Biol. Eng. Comp.* 33:235–237.

Wang, X.-B., Y. Huang, J. P. H. Burt, G. H. Markx, and R. Pethig. 1993. Selective dielectrophoretic confinement of bioparticles in potential energy wells. *J. Phys. D Appl. Phys.* 26:1278–1285.

Wang, X. B., J. Vykoukal, F. F. Becker, and P. R. C. Gascoyne. 1998. Separation of polystyrene microbeads using dielectrophoretic/gravitational field-flow fractionation. *Biophys. J.* 74:2689–2701.

Washizu, M., and O. Kurosawa. 1990. Electrostatic manipulation of DNA in microfabricated structures. *IEEE Trans. Ind. Appl.* 26:1165–1172.

Washizu, M., O. Kurosawa, I. Arai, S. Suzuki, and N. Shimamoto. 1995. Applications of electrostatic stretch-and-positioning of DNA. *IEEE Trans. Ind. Appl.* 31:447–456.

Washizu, M., S. Suzuki, O. Kurosawa, T. Nishizaka, and T. Shinohara. 1994. Molecular dielectrophoresis of biopolymers. *IEEE Trans. Ind. Appl.* 30:835–843.

Whitley, R. J. 1996. Fields' Virology. B. N. Fields et al., editors. Lippincott-Raven, Philadelphia. 2297–2342.